

Scientific Inquiry and Review (SIR)

Volume 7 Issue 1, 2023

ISSN (P): 2521-2427, ISSN (E): 2521-2435

Homepage: <https://journals.umt.edu.pk/index.php/SIR>



Article QR



Title: Transmission Analysis of Hepatitis B Epidemic Model using Standard and Non-standard Schemes

Author (s): Ihsan Ullah Khan¹, Muhammad Irfan¹, Azhar Iqbal², Amjid Hussain¹


Affiliation (s): ¹Gomal University, Dera Ismail Khan, KPK, Pakistan
²Dawood University of Engineering and Technology, Karachi, Pakistan

DOI: <https://doi.org/10.32350/sir.71.04>

History: Received: December 8, 2022, Revised: January 10, 2023, Accepted: January 10, 2023,
Published: March 15, 2023

Citation: Khan IU, Irfan M, Iqbal A, Hussain A. Transmission analysis of Hepatitis B epidemic model using standard and non-standard schemes. *Sci Inq Rev.* 2023;7(1):53–70. <https://doi.org/10.32350/sir.71.04>

Copyright: © The Authors

Licensing:  This article is open access and is distributed under the terms of [Creative Commons Attribution 4.0 International License](https://creativecommons.org/licenses/by/4.0/)

Conflict of Interest: Author(s) declared no conflict of interest



A publication of

The School of Science

University of Management and Technology, Lahore, Pakistan

Transmission Analysis of Hepatitis B Epidemic Model using Standard and Non-standard Schemes

Ihsan Ullah Khan^{1*}, Muhammad Irfan¹, Azhar Iqbal², and Amjid Hussain¹

¹Department of Mathematics, Institute of Numerical Sciences, Gomal University, Dera Ismail Khan, Pakistan

²Department of Mathematics, Dawood University of Engineering and Technology, Karachi, Pakistan

ABSTRACT

Mathematical modeling is a vast field that has interdisciplinary implications for research. These models help to investigate the basic dynamics and quantitative behavior of infectious diseases that affect human beings, such as COVID-19, hepatitis B virus (HBV), and human immunodeficiency virus (HIV). The current study investigates the spread of HBV by using the basic virus model. In order to determine the stability of disease-free and endemic equilibria, the basic reproduction number is determined. The convergence and divergence of disease-free and endemic equilibria are demonstrated by using standard finite difference (SFD) and non-standard finite difference (NSFD) schemes. Arguably, SFD schemes, namely Euler and Runge-Kutta order four (RK-4) schemes, converge for lower step sizes, while the NSFD scheme converges for all step sizes. The latter is a strong, efficient, and reliable method that shows a clear picture of the continuous model. All the results are validated using numerical simulations in order to better comprehend the dynamics of the disease. The theoretical and numerical findings in this work can be applied as a useful tool for tracking the prevalence of HBV infectious disease.

Keywords: convergence, divergence, HBV model, local and global stability, numerical schemes

1. INTRODUCTION

HBV is a devastating liver infection and an epidemic that poses a considerable health hazard, specifically in developing nations [1, 2]. HBV damages the liver and causes numerous shocking disorders. Almost 360 million people worldwide are affected by this infectious disease and among them are more than 150 million HBV transporters (who transmit the disease to healthy people) [3, 4]. Also, more than 150 million of them have chronic

* Corresponding Author: ihsanmrwt@gu.edu.pk

hepatitis C virus (HCV) infection and another 150–200 million are HBV chronic liver infection carriers [5]. HBV is transmitted by exposed sex, blood transfusion, and spreads into the recently born infant during pregnancy from the infected mother.

Mathematical models [6-19] are very useful for analyzing the dynamics of real-world problems. Researchers utilize ordinary differential equations [6-11] as well as partial differential equations [12-15] to investigate different characteristics of physical objects. Fractional order [16-19] mathematical models are also among the most investigated topics in the world in this regard. Mathematical modeling also helps in the analysis of experimental results, as well as understanding the fundamental biological mechanisms of disease transmission. Many mathematical models have been suggested to improve the understanding and knowledge of HBV disease. Zeuzem et al. [6] and Nowak et al. [7] recommended simple virus infection models in which clear immune responses are not required. These models are mostly applied in the analysis of virus infection dynamics. In [8], the author proposed and examined the stochastic SACR model for the transmission of HBV disease. In [9, 10], the authors focused on population characteristics, infectious diseases, infection characteristics, and related social factors of HBV. Aja et al. [11] constructed a model based on statistical data which is not only useful for forecasting disease transmission but also helps to identify the key factors that affect the disease spread.

In early 1980s, mathematical modelling was used to investigate the dynamics of HBV and the efficiency of disease control. To date, several systematic methods have been applied for the prevention of HBV transmission [20-22]. The most attractive and effective way of reducing the prevalence of HBV in newborns is vaccination. In case of vaccination, the emphasis shifts towards the use of a mathematical model to forecast the long-term consequences of immunization on hepatitis B regulation. Many scientists have analyzed the transmission mechanism of HBV and evaluated the effect of various vaccine policies [23, 24]. Recently, in [25], the author proposed and analyzed a non-linear basic adaptation system for HBV spread. The stability of disease-free and endemic equilibria was discussed for the continuous model. The author used a mathematical framework for the continuous model to study the stability of equilibria which strictly depend on the basic reproduction number.

The aim of the current study is to prevent the spread of HBV and explore its threats to the health of general people. Multiple numerical schemes, such as Euler, RK-4, and the NSFD scheme have been deployed to assess the various properties of the model and demonstrate their ecological feasibility and accuracy. The findings demonstrate that the aforementioned schemes give a thorough description of the continuous model.

The structure of the current paper is organized as follows. The HBV disease model and corresponding parameters are described in Section 2. In Section 3, the expression for R_0 , the equilibria of the system, and their stability are explored for the continuous model. SFD schemes, including Euler, RK-4, and the NSFD scheme are produced for the continuous model in Section 4. The fundamental dynamic properties of the continuous model containing the positivity of solutions cannot be preserved by Euler and RK-4 schemes for higher step sizes, leading to numerical solutions that are different from the solutions of the original system. However, the NSFD scheme gives positive solutions for all finite step sizes and basically overcomes the shortcomings of the SFD schemes. The analysis also demonstrates that the NSFD scheme is unconditionally convergent and provides better results in all aspects than Euler and RK-4 schemes. The theoretical findings are strengthened by numerical simulations at each stage. In Section 5, brief conclusions are offered to sum up the whole work.

2. INTRODUCTION OF HEPATITIS B DISEASE MODEL

Figure 1 depicts the non-linear basic HBV epidemic model [25].

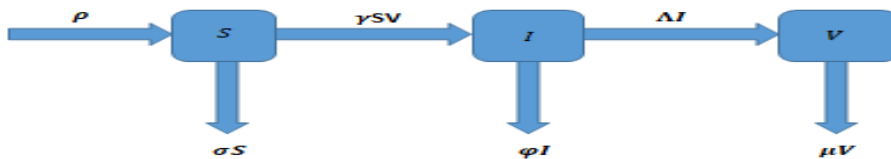


Figure 1. Illustration of Hepatitis B Disease Model

$$\begin{aligned}\frac{dS}{dt} &= \rho - \sigma S - \gamma SV, \\ \frac{dI}{dt} &= \gamma SV - \phi I, \\ \frac{dV}{dt} &= \Lambda I - \mu V.\end{aligned}\tag{2.1}$$

2.1. Parameters

The parameters used in system (2.1) are described as follows:

S	shows the number of uninfected cells in the population
I	shows the number of infected cells in the population
V	shows the number of free virus particles in the population
γ	shows the constant rate that explains the process reliability
ρ	shows the constant rate
Λ	shows the rate at which the virus leaves infected cells
σ	shows the die rate of uninfected cells
φ	shows how fast infected cells are dying
μ	shows a free virus

The parameters $\rho, \gamma, \sigma, \varphi, \Lambda, \mu$ are all positive constants.

3. STABILITY ANALYSIS OF CONTINUOUS MODEL (1) EQUILIBRIA

The following subsection gives the equilibria of model (1).

3.1. Equilibria of Model

If all other classes are equal to zero aside from the susceptible class, the above described system (2.1) has the disease-free equilibrium (DFE) point $E_0 = \left(\frac{\rho}{\sigma}, 0, 0\right)$. If the system (2.1) is solved simultaneously, then the endemic equilibrium (EE) point occurs which is $E^* = (S^*, I^*, V^*) = \left(\frac{\varphi\mu}{\gamma\Lambda}, \frac{\sigma\mu(R_0-1)}{\gamma\Lambda}, \frac{\sigma(R_0-1)}{\gamma}\right)$. In the following, R_0 is provided which is crucial for the stability of the equilibria of model (1).

3.2. Basic Reproductive Number (R_0)

The most essential threshold quantity for any infectious disease is R_0 . It helps to assess whether a contagious disease will spread among the people or not. R_0 is a significant biological quantity that may be determined using the modified technique known as the “next generation matrix” [26]. The transmission matrix $F(x)$ and translation matrix $V(x)$ for system (2.1) can be described as follows:

$$F(x) = \begin{bmatrix} \gamma SV \\ 0 \end{bmatrix} \text{ and } V(x) = \begin{bmatrix} \varphi I \\ -\Lambda I + \mu V \end{bmatrix}.$$

From the above, we can easily get

$$F = \begin{bmatrix} 0 & \frac{\gamma\rho}{\sigma} \\ 0 & 0 \end{bmatrix} \text{ and } V = \begin{bmatrix} \varphi & 0 \\ -\Lambda & \mu \end{bmatrix}.$$

As $R_0 = \rho(FV^{-1})$, so using the above information, R_0 becomes

$$R_0 = \frac{\gamma\rho\Lambda}{\mu\varphi\sigma}.$$

3.3. Stability of Equilibria

Theorem 3.1 [25]: The DFE point of system (2.1) is locally asymptotically stable (LAS) whenever $R_0 < 1$, as displayed in Figure 2(a).

Theorem 3.2 [25]: The EE point of system (1) is LAS whenever $R_0 > 1$, as displayed in Figure 2(b).

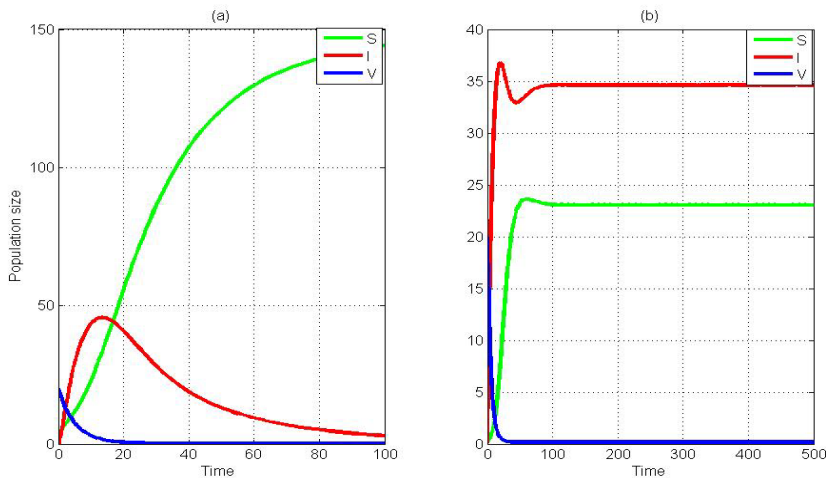


Figure 2. Numerical simulations for HBV model (1) with (a) $\gamma = .085$, (b) $\gamma = .85$. The remaining values of the parameters are offered as $\mu = .196$, $\sigma = .0667$, $\Lambda = .001$, $\varphi = .1$, $\rho = 10$.

According to the numerical simulations depicted in Figure 2(a), the DFE point of the continuous system (2.1) is stable if $R_0 < 1$. On the other hand, as illustrated in Figure 2(b), the EE point exists and becomes stable if $R_0 > 1$. It is evident from Figure 2 and the preceding discussion that the EE

point emerges and remains stable when the DFE point becomes unstable, that is, when R_0 passes the critical value $R_0 = 1$, the system exhibits transcritical bifurcation and stability exchange from one equilibrium point to another. It shows that $R_0=1$ is the saddle point for system (2.1). More details can be found in [25].

4. NUMERICAL ANALYSIS OF SYSTEM (1)

In the current section, different discrete schemes for the continuous model (1) are constructed. The main aim is to better understand the dynamics of HBV disease transmission. Three schemes, namely Euler, RK-4, and NSFD schemes [27, 28] are constructed. It is demonstrated that the NSFD scheme is not only independent of step size but also more preferable as compared to the other defined schemes in every aspect.

4.1. Euler Scheme

Subsequent steps can be employed to construct the Euler scheme for system (2.1).

$$\frac{S^{p+1} - S^p}{h} = \rho - \sigma S^p - \gamma S^p V^p$$

$$S^{p+1} - S^p = h[\rho - \sigma S^p - \gamma S^p V^p]$$

$$S^{p+1} = S^p + h[\rho - \sigma S^p - \gamma S^p V^p].$$

Similarly

$$\frac{I^{p+1} - I^p}{h} = \gamma S^p V^p - \phi I^p$$

$$I^{p+1} = I^p + h[\gamma S^p V^p - \phi I^p],$$

and

$$\frac{V^{p+1} - V^p}{h} = \Lambda I^p - \mu V^p,$$

$$V^{p+1} = V^p + h[\Lambda I^p - \mu V^p].$$

Therefore, the Euler scheme becomes

$$S^{p+1} = S^p + h[\rho - \sigma S^p - \gamma S^p V^p]$$

$$I^{p+1} = I^p + h[\gamma S^p V^p - \phi I^p] \tag{4.1}$$

$$V^{p+1} = V^p + h[\Lambda I^p - \mu V^p].$$

Once the step size is small, then the numerical solutions offered by the Euler scheme are positive, as illustrated in Figure 3(a-c). According to Figure 3(d), stability is disrupted as the step size increases. Therefore, the stability and positivity of Euler scheme does not maintain for all finite step sizes.

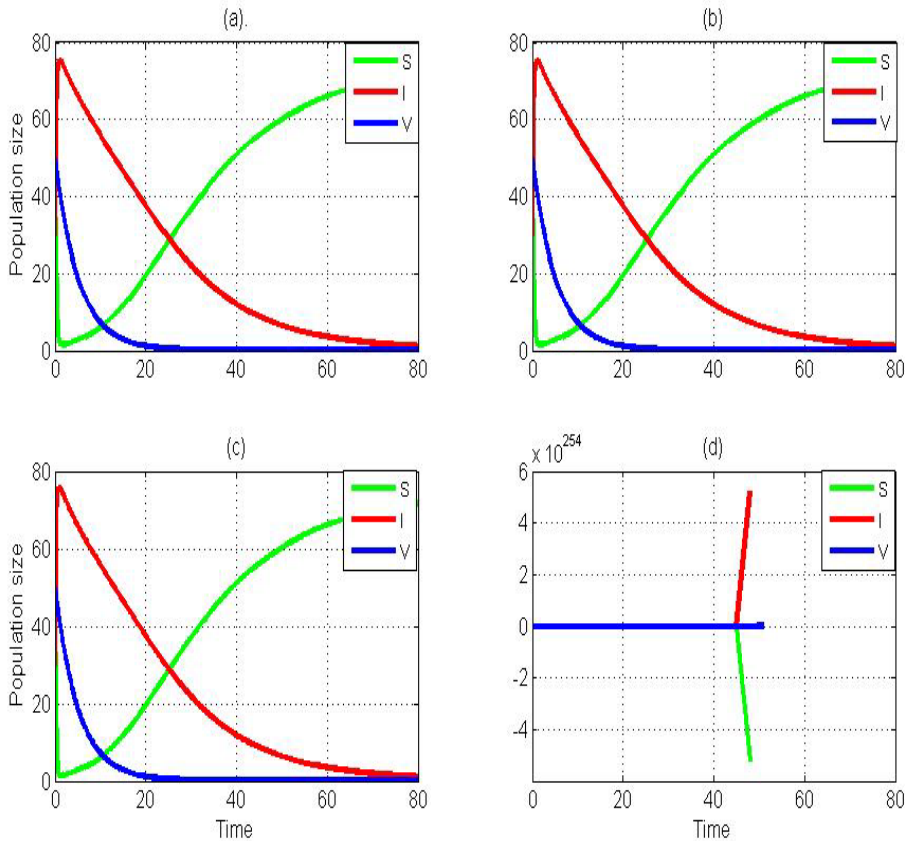


Figure 3. Graphs generated by Euler scheme (4.1) with (a) $h=0.001$, (b) $h=0.01$, (c) $h=0.1$ and (d) $h=3$. The remaining values of the parameters are offered as $\gamma = 0.085, \mu = 0.196, \sigma = 0.0667, \Lambda = 0.001, \varphi = 0.1, \rho = 10$.

4.2. Fourth-order Runge-Kutta Scheme (RK-4)

To develop the RK-4 scheme, it is assumed that $S = p_1, I = q_1$ and $V = r_1$. Then, the RK-4 scheme is described as follows:

Stage 1

$$p_1 = h[\rho - (d + \gamma V^p)S^p],$$

$$q_1 = h[\gamma S^p V^p - \varphi I^p],$$

$$r_1 = h[\Lambda I^p - \mu V^p].$$

Stage 2

$$p_2 = h\left[\rho - \left(\sigma + \gamma\left(V^p + \frac{r_1}{2}\right)\left(S^p + \frac{p_1}{2}\right)\right)\right],$$

$$q_2 = h\left[\gamma\left(V^p + \frac{r_1}{2}\right)\left(S^p + \frac{p_1}{2}\right) - \varphi\left(I^p + \frac{q_1}{2}\right)\right],$$

$$r_2 = h\left[\Lambda\left(I^p + \frac{q_1}{2}\right) - \mu\left(V^p + \frac{r_1}{2}\right)\right].$$

Stage 3

$$p_3 = h\left[\rho - \left(\sigma + \gamma\left(V^p + \frac{r_2}{2}\right)\left(S^p + \frac{p_2}{2}\right)\right)\right],$$

$$q_3 = h\left[\gamma\left(V^p + \frac{r_2}{2}\right)\left(S^p + \frac{p_2}{2}\right) - \varphi\left(I^p + \frac{q_2}{2}\right)\right],$$

$$r_3 = h\left[\Lambda\left(I^p + \frac{q_2}{2}\right) - \mu\left(V^p + \frac{r_2}{2}\right)\right].$$

Stage 4

$$p_4 = h[\rho - (\sigma + \gamma(V^p + r_3)(S^p + p_3))],$$

$$q_4 = h[\gamma(V^p + r_3)(S^p + p_3) - \varphi(I^p + q_3)],$$

$$r_4 = h[\Lambda(I^p + q_3) - \mu(V^p + r_3)].$$

Finally, we get

$$S^{p+1} = S^p + \frac{1}{6}[p_1 + 2p_2 + 2p_3 + p_4],$$

$$I^{p+1} = \frac{1}{6}[q_1 + 2q_2 + 2q_3 + q_4], \tag{4.2}$$

$$V^{p+1} = \frac{1}{6}[r_1 + 2r_2 + 2r_3 + r_4].$$

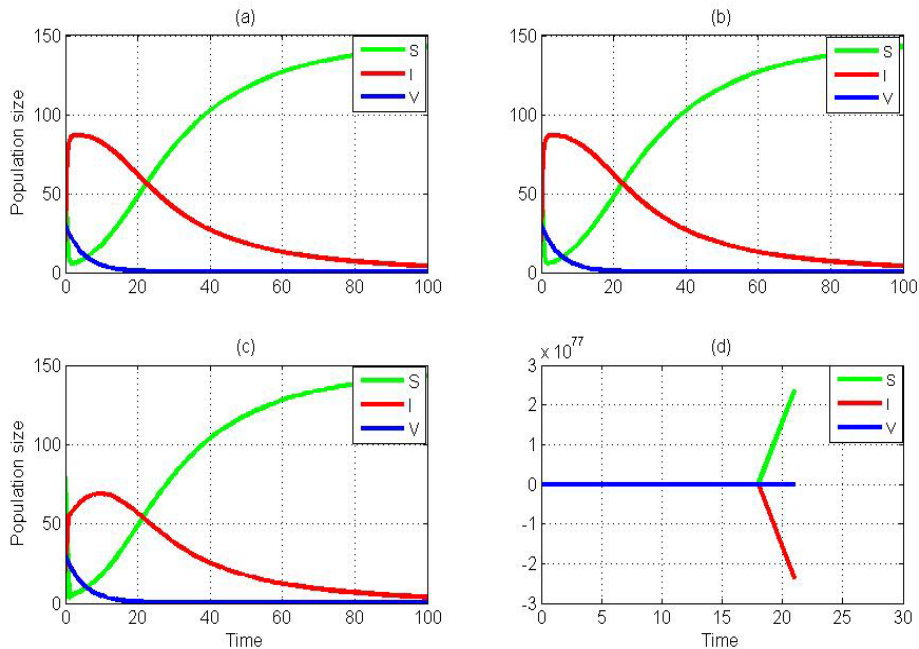


Figure 4. Graphs generated by RK-4 scheme (4.2) with (a) $h=0.01$, (b) $h=0.1$, (c) $h=1$ and (d) $h=3$. The remaining values of the parameters are offered as $\gamma = 0.085$, $\mu = .196$, $\sigma = .0667$, $\Lambda = .001$, $\varphi = 0.1$, $\rho = 10$.

Figure 4(a-d) provides a graphic representation of RK-4 scheme (4.2). The graphs produced by the RK-4 scheme are positive and convergent for small step sizes, as seen in Figure. 4(a-c). Figure 4(d) illustrates that the stability of model (1) is destroyed as the step size increases, that is, the RK-4 scheme diverges for large values of h .

4.3. Non-standard Finite Difference (NSFD) Scheme

Mickens [29] propagated the NSFD scheme which approximates the solutions of ordinary and partial differential equations. According to Shokri et al. [30], there are two factors that affect the study of the NSFD scheme. The first is how to discretize the derivative and the second constitutes the best way to approximate the nonlinear terms. The forward finite difference approximation is one of the general methods of first order derivative discretization. The first order derivative $\frac{dy}{dx}$ is written in standard form as $\frac{y(x+h)-y(x)}{h}$, where h stands for the step size. According to Mickens, this can

be expressed as $\frac{y(x+h)-y(x)}{\varphi(h)}$, where $\varphi(h)$ is referred to as the denominator function. There are various formulas for $\varphi(h)$ that can be viewed in [30]. In the current paper $\varphi(h) = h$. The following steps can be taken to construct the NSFD scheme for system (2.1).

$$\frac{S^{p+1} - S^p}{h} = \rho - \sigma S^{p+1} - \gamma S^{p+1} V^p,$$

$$\frac{I^{p+1} - I^p}{h} = \gamma S^p V^p - \varphi I^{p+1},$$

$$\frac{V^{p+1} - V^p}{h} = \Lambda I^p - \mu V^{p+1}.$$

The above equations can be rewritten as

$$\begin{aligned} S^{p+1} &= \frac{h\rho + S^p}{1 + h\sigma + h\gamma V^p}, \\ I^{p+1} &= \frac{I^p + h\gamma S^p V^p}{1 + h\varphi}, \\ V^{p+1} &= \frac{V^p + h\Lambda I^p}{1 + h\mu}. \end{aligned} \quad (4.3)$$

4.3.1. Investigating the Stability of Equilibria for the NSFD Scheme.

In order to discuss the local stability, suppose

$$\begin{aligned} F &= S^{p+1} = \frac{h\rho + S^p}{1 + h\sigma + h\gamma V^p}, \\ G &= I^{p+1} = \frac{I^p + h\gamma S^p V^p}{1 + h\varphi}, \\ H &= V^{p+1} = \frac{V^p + h\Lambda I^p}{1 + h\mu}. \end{aligned} \quad (4.4)$$

Theorem 4.1: The DFE point E_0 for the discrete NSFD scheme (4.3) is LAS if $R_0 < 1$.

Proof: Consider the Jacobean matrix

$$J = \begin{bmatrix} \frac{\partial F}{\partial S} & \frac{\partial F}{\partial I} & \frac{\partial F}{\partial V} \\ \frac{\partial G}{\partial S} & \frac{\partial G}{\partial I} & \frac{\partial G}{\partial V} \\ \frac{\partial H}{\partial S} & \frac{\partial H}{\partial I} & \frac{\partial H}{\partial V} \end{bmatrix}. \quad (4.5)$$

From (4.4), the following derivatives can be easily obtained

$$\frac{\partial F}{\partial S} = \frac{1}{(1+h\sigma+h\gamma V)}, \frac{\partial F}{\partial I} = 0, \frac{\partial F}{\partial V} = \frac{(h\rho+S)h\gamma}{[(1+h\sigma+h\gamma V)]^2}, \frac{\partial G}{\partial S} = \frac{\gamma hV}{(1+h\varphi)}, \frac{\partial G}{\partial I} = \frac{1}{(1+h\varphi)}, \frac{\partial G}{\partial V} = \frac{h\gamma S}{(1+h\omega)}, \frac{\partial H}{\partial S} = 0, \frac{\partial H}{\partial I} = \frac{h\Lambda}{1+h\mu}, \frac{\partial H}{\partial V} = \frac{1}{1+h\mu}.$$

By replacing all the above derivatives in (4.5), we obtain

$$J = \begin{bmatrix} \frac{1}{1+h\sigma+h\gamma V} & 0 & 0 \\ 0 & \frac{1}{1+h\varphi} & 0 \\ 0 & \frac{h\Lambda}{1+h\mu} & \frac{1}{1+h\mu} \end{bmatrix}.$$

Putting $E_0 = \left(\frac{\rho}{\sigma}, 0, 0\right)$, we obtain

$$J = \begin{bmatrix} \frac{1}{1+h\sigma} & 0 & 0 \\ 0 & \frac{1}{1+h\gamma} & 0 \\ 0 & \frac{h\Lambda}{1+h\mu} & \frac{1}{1+h\mu} \end{bmatrix}.$$

To verify the eigenvalues, we consider

$$|J(E_0) - \lambda I| = 0,$$

that is,

$$\begin{vmatrix} \frac{1}{1+h\sigma} - \lambda & 0 & 0 \\ 0 & \frac{1}{1+h\gamma} - \lambda & 0 \\ 0 & \frac{h\Lambda}{1+h\mu} & \frac{1}{1+h\mu} - \lambda \end{vmatrix} = 0. \tag{4.6}$$

System (4.6) has the following characteristic equation

$$\left(\frac{1}{1+h\sigma} - \lambda\right) \left(\lambda^2 + \left(\frac{1}{1+h\gamma} + \frac{1}{1+h\mu}\right)\lambda + (1 - R_0) \left(\frac{1}{(1+h\mu)(1+h\gamma)}\right)\right) = 0. \tag{4.7}$$

Using one of the eigenvalues from (4.7), $\lambda_1 = \frac{1}{1+h\sigma} < 1$ is obtained. The other two eigenvalues can be obtained from

$$\lambda^2 + \left(\frac{1}{1+h\gamma} + \frac{1}{1+h\mu}\right)\lambda + (1 - R_0) \left(\frac{1}{(1+h\mu)(1+h\gamma)}\right) = 0.$$

According to Routh Hurwitz criterion [31, 32], the roots of the above equation are less than one if $R_0 < 1$. As a result, the DFE point for the NSFD scheme is LAS.

Theorem 4.2: The EE point E^* for the discrete NSFD scheme (4.3) is LAS, if $R_0 > 1$.

Proof: In a manner analogous to **Theorem 4.1**, the Jacobian matrix is obtained as

$$J = \begin{bmatrix} \frac{\partial F}{\partial S} & \frac{\partial F}{\partial I} & \frac{\partial F}{\partial V} \\ \frac{\partial G}{\partial S} & \frac{\partial G}{\partial I} & \frac{\partial G}{\partial V} \\ \frac{\partial H}{\partial S} & \frac{\partial H}{\partial I} & \frac{\partial H}{\partial V} \end{bmatrix}. \quad (4.8)$$

By putting all the derivatives from **Theorem (4.1)**, the Jacobian matrix (4.8) becomes

$$J = \begin{bmatrix} \frac{1}{(1+h\sigma+h\gamma V)} & 0 & \frac{(h\rho+S)h\gamma}{[(1+h\sigma+h\gamma V)]^2} \\ \frac{\gamma h V}{(1+h\phi)} & \frac{1}{(1+h\phi)} & \frac{h\gamma S}{(1+h\phi)} \\ 0 & \frac{h\Lambda}{1+h\mu} & \frac{1}{1+h\mu} \end{bmatrix} \quad (4.9)$$

Furthermore, by replacing EE point E^* in matrix (4.9), we obtain

$$J(E^*) = \begin{bmatrix} \frac{1}{(1+h\sigma+h\gamma V^*)} & 0 & \frac{(h\rho+S^*)h\gamma}{[(1+h\sigma+h\gamma V^*)]^2} \\ \frac{\gamma h V^*}{(1+h\phi)} & \frac{1}{(1+h\phi)} & \frac{h\epsilon S^*}{(1+h\phi)} \\ 0 & \frac{h\Lambda}{1+h\mu} & \frac{1}{1+h\mu} \end{bmatrix}.$$

To check the eigenvalues, we take

$$|J(E^*) - \lambda I| = 0,$$

that is,

$$\begin{vmatrix} \frac{1}{(1+h\sigma+h\gamma V^*)} - \lambda & 0 & \frac{(h\rho+S^*)h\gamma}{[(1+h\sigma+h\gamma V^*)]^2} \\ \frac{\gamma h V^*}{(1+h\varphi)} & \frac{1}{(1+h\varphi)} - \lambda & \frac{h\gamma S^*}{(1+h\varphi)} \\ 0 & \frac{h\Lambda}{1+h\mu} & \frac{1}{1+h\mu} - \lambda \end{vmatrix} = 0. \tag{4.10}$$

From (4.10), $\lambda_1 = \frac{1}{(1+h\sigma+h\gamma V^*)}$ is obtained. The other two eigenvalues can be obtained from

$$\lambda^2 - \lambda \left(\frac{1}{(1+h\varphi)} + \frac{1}{1+h\mu} \right) - \left(\left(\frac{(h\rho+S^*)h\gamma}{(1+h\sigma+h\gamma V^*)^2} \times \frac{h\Lambda}{1+h\mu} \times \frac{\gamma h V^*}{(1+h\varphi)} \right) + \left(\frac{h\Lambda}{1+h\mu} \times \frac{\gamma h V^*}{(1+h\varphi)} \right) \right) (R_0 - 1) = 0. \tag{4.11}$$

The Routh Hurwitz criterion [31, 32] demonstrates that the roots of equation (4.11) are smaller than one if $R_0 > 1$. This demonstrates that E^* for the discrete NSFD scheme (4.3) is LAS whenever $R_0 > 1$.

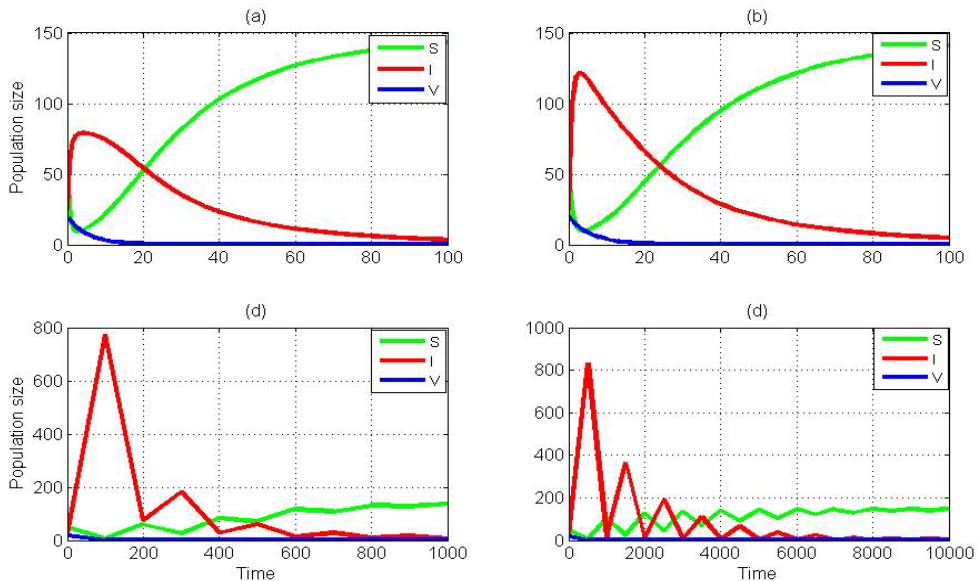


Figure 5. Graphs generated by the NSFD scheme (4.3) with (a) $h=0.1$, (b) $h=1$, (c) $h=100$ and (d) $h=500$. The remaining values of the parameters are offered as $\gamma = .085, \mu = 0.196, \sigma = .0667, \Lambda = .001, \varphi = 0.1, \rho=10$.

Figure 5(a-d) depicts that the NSFD scheme (4.3) remains stable for each step size. The SFD scheme, however, shows convergence for lower step sizes. This demonstrates that for each step size the NSFD scheme is positive forever and unconditionally convergent.

5. CONCLUSION

The basic disease model for HBV has been proposed and examined in the current paper. For the proposed epidemic system, the equilibria and threshold quantity R_0 have been determined. In order to verify the convergence and divergence of the DFE and EE points, various numerical approaches have been employed. It has been demonstrated that RK-4 and Euler schemes depend on step sizes and are conditionally convergent which makes them ineffective. On the other hand, the NSFD approach developed for the current model is not step size dependent. This shows that the NSFD scheme is incredibly effective in comparison to the notable Euler and RK-4 numerical schemes. This scheme is a simple technique that demonstrates how discrete and continuous models behave appropriately and provide mathematically accurate results. By employing it, the spread of HBV epidemic diseases can be monitored effectively. The findings presented in this paper are beneficial to humanity in the field of medicine and can be applied also as a useful tool to predict the appearance of HBV epidemic disease. Each section includes numerical simulations to validate the theoretical findings.

REFERENCES

1. Kamyad AV, Akbari R, Heydari AA, Heydari A. Mathematical modeling of transmission dynamics and optimal control of vaccination and treatment for Hepatitis B virus. *Comput Math Methods Med.* 2014;2014:e475451. <https://doi.org/10.1155/2014/475451>
2. Gentile I, Borgia G. Vertical transmission of Hepatitis B virus: Challenges and solutions. *Int J Women's Health.* 2014;6:605–611. <http://dx.doi.org/10.2147/IJWH.S51138>
3. Sirilert S, Trairisilp K, Sirivatanapa P, Tongsong T. Pregnancy outcomes among chronic carriers of Hepatitis B virus. *Int J Gynaecol Obstet.* 2014;126(2):106–110. <https://doi.org/10.1016/j.ijgo.2014.02.019>
4. World Health Organization. Prevention and control of viral hepatitis infection: Framework for global action. No. WHO/HSE/PED/HIP/GHP

- 2012.1. World Health Organization. <https://apps.who.int/iris/handle/10665/130012>. 2012.
5. Zou L, Zhang W, Ruan S. (2010). Modeling the transmission dynamics and control of Hepatitis B virus in China. *J Theor Biol.* 2010;262(2):330–338. <https://doi.org/10.1016/j.jtbi.2009.09.035>
 6. Zeuzem S, Schmidt JM, Lee J, Ruster B, Roth WK. Effect of interferon alfa on the dynamics of Hepatitis C virus turnover in vivo. *Hepatology.* 1996;23(2):366–371. <https://doi.org/10.1002/hep.51023025>
 7. Nowak MA, Bangham CR. Population dynamics of immune responses to persistent viruses. *Science.* 1996;272(5258):74–79. <https://doi.org/10.1126/science.272.5258.74>
 8. Khan A, Hussain G, Zahri M, Zaman G, Humphries UW. A stochastic SACR epidemic model for HBV transmission. *J Biol Dyn.* 2020;14(1):788–801. <https://doi.org/10.1080/17513758.2020.1833993>
 9. Nakata Y, Kuniya T. Global dynamics of a class of SEIRS epidemic models in a periodic environment. *J Math Anal Appl.* 2010;363(1):230–237. <https://doi.org/10.1016/j.jmaa.2009.08.027>
 10. Hethcote HW. The mathematics of infectious diseases. *SIAM Rev Soc Ind Appl Math.* 2000;42(4):599–653. <https://doi.org/10.1137/S0036144500371907>.
 11. Aja RO, Omale D. Stability analysis of the transmission dynamics of Hepatitis B virus infection with controls in a population. *Int J Adv Math.* 2018;2018(6):52–63.
 12. Iqbal MS, Yasin MW, Ahmed N, Akgül A, Rafiq M, Raza A. Numerical simulations of nonlinear stochastic Newell-Whitehead-Segel equation and its measurable properties. *J Comput Appl Math.* 2023;418:e114618. <https://doi.org/10.1016/j.cam.2022.114618>
 13. Bilal S, Shah IA, Akgül A, Tekin MT, Botmart T, Yahia IS. A comprehensive mathematical structuring of magnetically effected Sutterby fluid flow immersed in dually stratified medium under boundary layer approximations over a linearly stretched surface. *Alexandria Eng J.* 2022;61(12):11889–11898. <https://doi.org/10.1016/j.aej.2022.05.044>
 14. Qureshi ZA, Bilal S, Khan U, et al. Mathematical analysis about influence of Lorentz force and interfacial nano layers on nanofluids flow through orthogonal porous surfaces with injection of SWCNTs. *Alexandria Eng J.* 2022;61(12):12925–12941. <https://doi.org/10.1016/j.aej.2022.07.010>

15. Shah IA, Bilal S, Akgül A, et al. On analysis of magnetized viscous fluid flow in permeable channel with single wall carbon nano tubes dispersion by executing nano-layer approach. *Alexandria Eng J.* 2022;61(12):11737–11751. <https://doi.org/10.1016/j.aej.2022.05.037>
16. Modanli M, Göktepe E, Akgül A, Alsallami SA, Khalil EM. Two approximation methods for fractional order Pseudo-Parabolic differential equations. *Alexandria Eng J.* 2022;61(12):10333–10339. <https://doi.org/10.1016/j.aej.2022.03.061>
17. Farman M, Akgül A, Tekin MT, et al. Fractal fractional-order derivative for HIV/AIDS model with Mittag-Leffler kernel. *Alexandria Eng J.* 2022;61(12):10965–10980. <https://doi.org/10.1016/j.aej.2022.04.030>
18. Attia N, Akgül A, Seba D, Nour A, Asad J. A novel method for fractal-fractional differential equations. *Alexandria Eng J.* 2022;61(12):9733–9748. <https://doi.org/10.1016/j.aej.2022.02.004>
19. Xu C, Farman M, Hasan A, et al. Lyapunov stability and wave analysis of Covid-19 omicron variant of real data with fractional operator. *Alexandria Eng J.* 2022;61(12):11787–11802. <https://doi.org/10.1016/j.aej.2022.05.025>
20. Zhao S, Xu Z, Lu Y. A mathematical model of Hepatitis B virus transmission and its application for vaccination strategy in China. *Int J Epidemiol.* 2000;29(4):744–752. <https://doi.org/10.1093/ije/29.4.744>
21. Gupta E, Bajpai M, Sharma P, Shah A, Sarin SK. Unsafe injection practices: A potential weapon for the outbreak of blood borne viruses in the community. *Ann Med Health Sci Res.* 2013;3(2):177–181. <https://doi.org/10.4103/2141-9248.113657>
22. Kabir KA, Kuga K, Tanimoto J. Analysis of SIR epidemic model with information spreading of awareness. *Chaos Solitons Fractals.* 2019;119:118–125. <https://doi.org/10.1016/j.chaos.2018.12.017>
23. Blumberg BS. *Hepatitis B: The Hunt for a Killer Virus.* United States of America: Princeton University Press; 2002. <https://doi.org/10.1086/376070>
24. McLean AR, Blumberg BS. Modelling the impact of mass vaccination against hepatitis B. I. Model formulation and parameter estimation. *Biol Sci.* 1994;256(1345):7–15. <https://doi.org/10.1098/rspb.1994.0042>
25. Khatun Z, Islam MS, Ghosh U. Mathematical modeling of Hepatitis B virus infection incorporating immune responses. *Sensors Int.* 2020;1:e100017. <https://doi.org/10.1016/j.sintl.2020.100017>

26. Van den Driessche P, Watmough J. Reproduction numbers and sub-threshold endemic equilibria for compartmental models of disease transmission. *Math Biosci.* 2002;180(1-2):29–48. [https://doi.org/10.1016/S0025-5564\(02\)00108-6](https://doi.org/10.1016/S0025-5564(02)00108-6)
27. Mickens RE. Calculation of denominator functions for nonstandard finite difference schemes for differential equations satisfying a positivity condition. *Numer Methods Partial Differ Equ.* 2007;23(3):672–691. <https://doi.org/10.1002/num.20198>
28. Lambert JD. *Numerical methods for ordinary differential systems: The initial value problem.* New York: John Wiley & Sons, Inc; 1991.
29. Mickens RE. *Nonstandard finite difference models of differential equations.* World Scientific Publishing; 1993.
30. Shokri A, Khalsaraei MM, Molayi M. Nonstandard dynamically consistent numerical methods for MSEIR Model. *J Appl Comput Mech.* 2022;8(1):196–205. <https://doi.org/10.22055/jacm.2021.36545.2863>
31. Ucakan Y, Gulen S, Koklu K. Analysing of tuberculosis in Turkey through SIR, SEIR and BSEIR Mathematical Models. *Math Comput Model Dyn Syst.* 2021;27(1):179–202. <https://doi.org/10.1080/13873954.2021.1881560>
32. Khan MA, Badshah Q, Islam S, Khan I, Shafie S, Khan SA. Global dynamics of SEIRS epidemic model with non-linear generalized incidences and preventive vaccination. *Adv Differ Equ.* 2015:e88. <https://doi.org/10.1186/s13662-015-0429-3>